

## Supporting Information

### Average Orientation of a Molecular Rotor Embedded in a Langmuir-Blodgett Monolayer

Deborah L. Casher,<sup>a</sup> Lukáš Kober,<sup>a</sup> and Josef Michl<sup>a,b\*</sup>

<sup>a</sup> Department of Chemistry and Biochemistry, University of Colorado, Boulder, Colorado 80309-0215, U.S.A., and

<sup>b</sup> Institute of Organic Chemistry and Biochemistry, Academy of Sciences of the Czech Republic, Flemingovo nám. 2, Prague 16610, Czech Republic

#### Table of Contents

Orientation Determination	S2
Synthesis	S2
Sample Preparation	S3
Ellipsometry	S4
Polarized Emission and Excitation	S5
Computational Methods	S5
FT-IR Spectroscopy	S5
Calculated Vibrational Spectrum of <b>4</b>	S11
Fitted Spectra	S14
Figure 1S	S14
References	S16

## Orientation Determination

Averaged over the sample, the probability of absorption is  $|\mathbf{M}_f|^2 K_f$ , where  $K_f = \langle \cos^2 fZ \rangle$ ,  $fZ$  is the angle that  $\mathbf{M}_f$  makes with  $Z$ , and the pointed brackets indicate an ensemble average. The orientation factor  $K_f$  of the  $f$ -th transition reflects both the alignment of its transition moment within an arbitrarily chosen molecular framework  $x'y'z'$  and the orientation of this framework with respect to surface normal  $Z$ . We assume that the sample is uniaxial with  $Z$  as the unique axis and work with the molecular framework  $xyz$  defined by the principal orientation axes. These are the axes in which the orientation tensor  $K_{uv} = \langle \cos uZ \cos vZ \rangle$  is diagonal. The orientation of the principal framework of axes is characterized by the three diagonal orientation factors  $K_u = \langle \cos^2 uZ \rangle$  ( $u = x, y, z$ ). We have simplified  $K_{uu}$  to  $K_u$  and chosen the axis labels such that  $K_z > K_y > K_x$  ( $z$  is often referred to as “the orientation axis”). Only two of the orientation factors  $K_u$  are independent since  $\sum_u K_u = 1$  follows from the properties of direction cosines.

## Synthesis

Anhydrous dichloromethane, triethylamine and acetonitrile were distilled from calcium hydride. All reactions were conducted under a dry argon atmosphere using Schlenk techniques unless otherwise noted. IR spectra were recorded with a Nicolet Avatar 360 FT-IR spectrophotometer. UV-Vis spectra were recorded on a Hewlett-Packard 8452A spectrophotometer. NMR spectra were recorded with an Inova 400 spectrometer or Bruker Avance-III 300 Spectrometer. A Hewlett-Packard 5989B mass spectrophotometer was used to record mass spectra. Elemental analyses were performed by Columbia Analytical Services, Tucson AZ.

**1-Naphthyltris(15-carboxypentadec-1-yloxy)silane (1):** A dried Schlenk flask (50

mL), equipped with a septum and magnetic stir bar, was charged with 1-naphthyltrichlorosilane (1.00 g, 3.822 mmol, 1.0 equiv.) and 16-hydroxyhexadecanoic acid (3.124 g, 11.467 mmol, 3.0 equiv.), and it was evacuated and filled with argon three times. Anhydrous dichloromethane (30 mL) and anhydrous triethylamine (1.161 g, 11.467 mmol, 3.0 equiv.) were added to the mixture and it was stirred at room temperature for 2 days. It was then filtered under argon, the filtrate was washed with anhydrous dichloromethane ( $2 \times 20$  mL), and the solvent was removed under reduced pressure. The crude product was purified by repeated crystallization from anhydrous acetonitrile to yield 1.485 g (40 %) of white crystals, mp ( $\text{CH}_2\text{Cl}_2$ ) 66 °C.  $^1\text{H}$  NMR (300 MHz,  $\text{CD}_2\text{Cl}_2$ ) 8.30 (dd,  $J = 8.1, 1.6$  Hz, 1H), 7.96 (dd,  $J = 6.8, 1.3$  Hz, 1H), 7.94 - 7.89 (m, 1H), 7.87 - 7.82 (m, 1H), 7.54 - 7.43 (m, 3H), 3.80 (t,  $J = 6.6$  Hz, 6H), 2.33 (t,  $J = 7.4$  Hz, 6H), 1.76 - 1.51 (m, 12H), 1.49 - 1.14 (m, 66H).  $^{13}\text{C}\{^1\text{H}\}$  NMR (75 MHz,  $\text{CD}_2\text{Cl}_2$ ) 180.07, 137.55, 136.54, 133.80, 131.44, 130.07, 129.23, 129.08, 126.67, 126.10, 125.49, 63.65, 34.43, 33.00, 30.22, 30.19, 30.18, 30.15, 30.10, 29.94, 29.91, 29.75, 29.51, 26.35, 25.23. IR (KBr,  $\text{cm}^{-1}$ ): 718, 774, 796, 832, 912, 948, 987, 1021, 1082, 1093, 1151, 1201, 1218, 1243, 1280, 1297, 1389, 1409, 1432, 1465, 1504, 1705, 2678, 2848, 2918, 3035, 3052. UV-Vis ( $\text{CH}_2\text{Cl}_2$ , nm)  $\lambda_{\text{max}}$  ( $\epsilon_{\text{max}}$ ): 227 (62500), 264 (4400), 274 (6700), 284 (7900), 296 (5500). MS (ESI $^+$ ): 991.7 (calcd. for  $\text{MNa}^+$ : 991.7). Elemental analysis: Calcd. C: 71.85 %, H: 10.40 %. Found: C: 71.64 %, H: 10.56 %.

### Sample Preparation

Si-SiO<sub>2</sub> wafers were cleaned in a freshly prepared piranha solution of 30% H<sub>2</sub>O<sub>2</sub>:conc. H<sub>2</sub>SO<sub>4</sub> (1:1 v:v) for 30 min, followed by rinsing with water. SiO<sub>2</sub> substrates were cleaned in an O<sub>2</sub> plasma

cleaner/sterilizer (Harrick, PDC-3XG) for 2-5 min, followed by soaking in 2-propanol for 5-10 min. Both cleaning methods resulted in hydrophilic surfaces that were fully wetted by water. Following cleaning, substrates were dried in a stream of N<sub>2</sub> or Ar and immediately immersed into the clean, water-filled Langmuir trough (SiO<sub>2</sub>) or, in the case of Si-SiO<sub>2</sub>, characterized by ellipsometry, re-rinsed and dried, and immersed into the trough within 10 min of the initial cleaning. Following the deposition, Films sat untouched for 15-20 min before removal for ellipsometric (on Si-SiO<sub>2</sub> only) and subsequent spectroscopic measurements. Between measurements, samples were stored in capped glass vials.

### Ellipsometry

A three-phase model, for Si, SiO<sub>2</sub>, and air, was used in the thickness calculation of the native oxide layer (SiO<sub>2</sub>) with the following parameters:<sup>1</sup>  $n = 3.858$ ,  $k = 0.018$  for Si,  $n = 1.462$ ,  $k = 0$  for SiO<sub>2</sub> and  $n = 1$ ,  $k = 0$  for air, where  $n$  is the refractive index and  $k$  is the extinction coefficient at the wavelength of the ellipsometer source. The same model was used to calculate film thickness with  $n = 1.462$ ,  $k = 0$ . Uncertainty in the ellipsometric thickness of pure films of **1a** and **2a** is based on averages of three or more films. For mixed films, thickness  $t$  is reported as the difference between the average film thickness on SiO<sub>2</sub> and the average thickness of SiO<sub>2</sub> for an individual sample, and the uncertainty  $\sigma$  is given by:

$$\sigma(t_{\text{SAM}}) = ([S(t_{\text{SiO}_2})]^2 + [S(t_{\text{SAM} + \text{SiO}_2})]^2)^{1/2}, \quad (1)$$

where  $S$  is the sample standard deviation.

## Polarized Emission and Excitation

Polarized spectra were measured with the polarizer transmission directions in four configurations: both horizontal (HH), both vertical (VV), excitation horizontal and emission vertical (HV), and vice versa (VH). Spectra were corrected for the wavelength dependent lamp output and detection efficiency and by a factor of  $\lambda^2$  for conversion to wavenumbers.<sup>2</sup> The derivation of the equation for calculating the steady state anisotropy,  $r_0$ , for any angle between the excitation light and the collection optics may be found in Gallivan et al.<sup>3</sup>

## Computational Methods

To evaluate the reliability of the calculated transition moment directions of **4** and their absolute orientation in the molecular coordinate system defined by the naphthalene ring, we calculated the vibrational spectrum of propene ( $\text{CH}_2=\text{CHCH}_3$ ) using the same method described for **4** for comparison with the MP2/CCSD/6-311G(d,p) calculated transition moment directions for propene reported previously.<sup>4</sup>

## FT-IR Spectroscopy

Figure 4A in the main text shows the alkyl C-H stretching region of **1**, **1a**, **2a**, and mixed films, with spectra normalized to the asymmetric  $\text{CH}_2$  band. The spectrum of **1** in KBr has been baseline corrected to eliminate the broad wings from H-bonded O-H stretching. The asymmetric and symmetric  $\text{CH}_2$  bands appear, respectively, around 2916 and 2849  $\text{cm}^{-1}$  in spectra of **1**, **1a**, and **2a**, consistent with an all-*trans* arrangement of the alkyl chains.<sup>5</sup> In contrast, spectra of mixed

monolayers show CH<sub>2</sub> bands shifted to higher frequencies at ~2926 cm<sup>-1</sup> and 2853 cm<sup>-1</sup>, which are associated with *gauche*-defects and increased disorder in the alkyl chains. The full width at half-maximum (FWHM) of the asymmetric CH<sub>2</sub> band is smallest in the monolayer spectra of **1a** and **2a** (20-24 cm<sup>-1</sup>), somewhat larger in the mixed films (~28 cm<sup>-1</sup>), and greatest in the spectrum of **1** in KBr (~46 cm<sup>-1</sup>), although the latter is likely distorted by H-bonded O-H stretching. A similar trend is seen for the FWHMs of the symmetric CH<sub>2</sub> band. All of the monolayer spectra show a decrease in the symmetric CH<sub>2</sub> band intensity compared to spectra in KBr when normalized to the asymmetric CH<sub>2</sub> band (Figure 4A), although given the distortion in this region due to O-H stretching in KBr the significance of this intensity difference remains uncertain. The inset of Figure 4A, which shows the relative intensities of the monolayer spectra in this region, reveals that the CH<sub>2</sub> bands in the single component films of **1a** and **2a** are much less intense relative to their counterparts in the mixed films.

Figure 4B in the main text shows bands associated with carbonyl stretching (1740-1700 cm<sup>-1</sup>), carboxylate asymmetric (1562-1536 cm<sup>-1</sup>) and symmetric (~1430 cm<sup>-1</sup>) stretching (in the monolayer films only), and C-H deformation around 1468 cm<sup>-1</sup> in spectra of **1**, **1a**, **2a**, and mixed films. For clarity, the monolayer film intensities are shown relative to one another and the C=O band of **1** in KBr has been normalized to that in the 11.5:1 mixed film.

The stretching frequency of the C=O band is sensitive to the degree of hydrogen-bonding to the carbonyl oxygen atom<sup>6</sup> and overlapping bands centered around 1738 and 1721 cm<sup>-1</sup> in the spectrum of **1a** are consistent with non hydrogen bonded and singly hydrogen bonded C=O oxygen atoms, respectively. In **1** (in KBr), **2a**, and mixed films, the C=O stretching band is centered around 1700 cm<sup>-1</sup>, which is associated with doubly H-bonded carbonyl oxygen atoms.<sup>6</sup>

In all of these spectra, the C=O band is quite broad and encompasses much of the region between 1740-1700  $\text{cm}^{-1}$ , suggesting that a multitude of H-bonded configurations have been formed in each sample.

A broad, intense band centered around 1562  $\text{cm}^{-1}$  in spectra of **2a** and mixed films is assigned to the asymmetric  $\text{COO}^-$  stretch.<sup>7</sup> The spectrum of **1a** has a band (or bands) centered around 1542-1536  $\text{cm}^{-1}$  with a possible weak shoulder around 1562  $\text{cm}^{-1}$ . All of the monolayer spectra show an intense, broad band around 1429  $\text{cm}^{-1}$  which is assigned to the  $\text{COO}^-$  symmetric stretch coupled with acid O-H deformation. Overlapping methylene C-H deformation bands fall between 1468 and 1370  $\text{cm}^{-1}$ .<sup>8a</sup> Of the methylene deformation bands, a narrow, sharp singlet around 1468  $\text{cm}^{-1}$  in monolayer films, as observed in the spectrum of **1a**, has been attributed to a cylindrically symmetrical, hexagonal packing arrangement of hydrocarbon chains in LB films.<sup>6,9,10</sup> A somewhat broader absorbance between  $\sim 1467$ -1457  $\text{cm}^{-1}$ , which appears as a shoulder on the intense  $\text{COO}^-$  band, as observed in spectra of **2a** and mixed films, is more difficult to interpret. Methylene doublets observed at 1472, 1464  $\text{cm}^{-1}$  and 730, 720  $\text{cm}^{-1}$  in the spectra of **1** and **2** in KBr (see Table 2 in the main text) have been reported in spectra of multilayer films.<sup>11,12</sup> Based on the frequency differences with the former and the absence of a methylene rocking doublet at 730, 720  $\text{cm}^{-1}$  in the monolayer spectrum of **2a**, the band at  $\sim 1467$ -1457  $\text{cm}^{-1}$  is unlikely to be related to the doublet seen in multilayer films.

The intensity of the spectrum of **1a** from 1800 to 1400  $\text{cm}^{-1}$  is notably weaker compared to the other monolayer films (as also observed in the alkyl C-H stretching region discussed above). However, relative to the C=O band, the  $\text{COO}^-$  bands are only slightly weaker than they appear in mixed films and in the spectrum of **2a**, suggesting that the absolute intensity of **1a** in this

region is a result of the different environment, and perhaps a different orientation, of the C=O and COO<sup>-</sup> head groups compared to the other films.

Naphthalene and naphthalenes substituted in the 1-position have several characteristic bands in the IR that may be distinguished from absorptions associated with the chains of **1** and **1a**: C-H stretching bands between 3110 and 3000 cm<sup>-1</sup>,<sup>13</sup> C=C stretching bands between 1620 and 1505 cm<sup>-1</sup>,<sup>8b</sup> and out-of-plane (oop) C-H bending bands between 865 and 775 cm<sup>-1</sup>.<sup>14,15</sup> Figure 4C-D in the main text shows these regions of the spectrum of **1** in KBr and monolayer spectra of **1a** and **2a-1a** (5.3:1). Ring bands in the spectrum of the 11.5:1 mixed film are not shown as they were too weak to interpret reliably.

The aromatic C-H stretching region in Figure 4C shows two or more overlapping bands centered around 3060 and 3042 cm<sup>-1</sup> in both the KBr and monolayer spectra. Similar bands have been reported in spectra of 1-alkylnaphthalenes.<sup>15</sup> Two weaker bands which are also known<sup>13</sup> in spectra of naphthalenes and 1-alkylnaphthalenes around 3100-3075 cm<sup>-1</sup> and 3020-3000 cm<sup>-1</sup> are not clearly observed in any of our spectra. Determination of the intensities of the bands observed for **1** and films containing **1a** is complicated by the degree of overlap and, furthermore, by the intense OH bands (which we have crudely attempted to subtract out) in the KBr spectrum and significant noise in the monolayer spectra. Despite these limitations, there does appear to be some enhancement of the high energy side of the 3060 cm<sup>-1</sup> band in both of the monolayer spectra relative to the KBr spectrum.

Figure 4D in the main text shows C=C stretching frequencies between 1620 and 1505 cm<sup>-1</sup> along with C-H out-of-plane (oop) bending bands from 833 to 775 cm<sup>-1</sup>. The spectrum of **2a** on Si-SiO<sub>2</sub> and that of (1-phenyl)triethoxysilane (**5**) in the region from 850 to 750 cm<sup>-1</sup> are also



shown for reasons discussed below. In the spectrum of **1** in KBr, C=C bands are observed at 1619, 1589, 1569, and 1505  $\text{cm}^{-1}$ , similar to frequencies reported in the spectrum of naphthalene and 1-substituted naphthalenes.<sup>8b,14</sup> While the highest energy of these bands is not apparent above the noise in either of the monolayer spectra, the other bands are observed, albeit somewhat distorted by the broad, intense underlying asymmetric  $\text{COO}^-$  stretch apparent in Figure 3 in the main text. In order to separate the ring bands from the  $\text{COO}^-$  stretch we used correction curves obtained by hand which gave reproducible intensities for the relatively intense bands around 1590 and 1505  $\text{cm}^{-1}$  while the intensity of the weak band around 1570  $\text{cm}^{-1}$  was somewhat more variable. Typical results for the corrected curves are shown in Figure 4D in the main text.

In the oop bending region, three intense bands are observed around 833, 798, and 776  $\text{cm}^{-1}$  in all of the spectra as seen in Figure 4D. Spectra of **2a** and **5** are included in Figure 4D to show absorption bands that likely contribute in this region that are not due to the naphthalene ring. While **2a** does not have any band structure in this region, it has a broad underlying absorbance, likely due to the Si-SiO<sub>2</sub> wafer, which presumably similarly affects the other monolayer samples. In the spectrum of **5**, two bands are apparent in this region: a broad band at 786  $\text{cm}^{-1}$  with an intense shoulder around 810  $\text{cm}^{-1}$ . Intense oop phenyl ring bands (not shown) appeared at 739 and 701  $\text{cm}^{-1}$  in our spectra, consistent with reports<sup>8c</sup> for monosubstituted benzenes, so it is likely that the bands observed at 786 and 810  $\text{cm}^{-1}$  are associated with all or part of the SiOCH<sub>2</sub>- group and therefore may be expected to contribute to the spectra of **1** and **1a**.

In Figure 4D, the oop ring band region in the monolayer spectra has been corrected by scaling the spectra of **2a** and **5** and then subtracting maximum intensity of each from the monolayer spectra that still resulted in a non-negative baseline. The spectrum of **1** in KBr was

corrected with the spectrum **5** only. In the main part of the figure, the corrected spectra of **1** in KBr and **1a** on Si-SiO<sub>2</sub> are shown normalized to the most intense band around 775 cm<sup>-1</sup>. The inset shows spectra of **1** and the mixed film normalized to this same band. In both cases, the band widths in KBr and in the monolayer spectra are similar at 775 cm<sup>-1</sup>. Bands at 833 and 797 cm<sup>-1</sup> in the monolayer spectrum of **1a** are slightly weaker and have somewhat smaller band widths compared to their counterparts in KBr. The mixed monolayer film (Figure 4D, Inset) shows a significantly weakened and narrower band at 799 cm<sup>-1</sup> and a somewhat more intense but narrower band at 832 cm<sup>-1</sup> compared to the KBr spectrum.

There are many other bands associated with the naphthalene ring between 1500 and 900 cm<sup>-1</sup> that overlap with and are generally obscured by other, more intense bands. The most intense of these ring bands appear at 1152-1146, 1025, and 992-990 cm<sup>-1</sup>, and while they are observed in the monolayer spectra it is difficult to get reasonable baselines and intensities of these bands due to the degree and different kinds of overlap that occur in each spectrum. For example, Figure 3 shows that the intense SiO<sub>2</sub> bands (due to differences in the blank and sample substrates<sup>16</sup>) around 1230 and 1085-1040 cm<sup>-1</sup> appear with very different intensities in each of the monolayer samples. These bands, along with the very strong SiOCH<sub>2</sub> band<sup>8d</sup> observed at 1085 cm<sup>-1</sup> in the spectrum of **1** in KBr, obscure all of the intense ring bands in this region, making reliable baseline determination an arduous if not impossible task. It is also not feasible to assign meaningful intensities to less intense ring bands between 1085-1040 cm<sup>-1</sup>, 1035-1011 cm<sup>-1</sup>, and at 1000 cm<sup>-1</sup> which have been identified with the naphthalene ring based on calculations (discussed below) and spectra of 1-substituted naphthalenes.<sup>13</sup> The increasingly poor signal-to-noise ratio in the region below ~710 cm<sup>-1</sup> obscures this region from interpretation.

## Calculated Vibrational Spectrum of 4

Starting with the highest energy ring bands shown in Figure 4C in the main text, 7 aromatic C-H stretching frequencies are calculated to lie in this region. The calculated band at  $3111\text{ cm}^{-1}$  is assigned to a weak, mostly  $y$  axis polarized band that has been observed in the spectra of some 1-alkyl substituted naphthalenes around  $3110\text{ cm}^{-1}$ .<sup>15</sup> While the spectrum of **1** in KBr has some band structure in this region, it is too weak to be distinguished from the underlying associated acid O-H stretching. None of the monolayer samples show any bands above the noise in this region. The next three bands associated with aromatic C-H stretching are assigned to the experimental band observed around  $3060\text{ cm}^{-1}$ . The highest energy band among these, at  $3067\text{ cm}^{-1}$ , is calculated to be the weakest of the three and has its transition moment closest to molecular  $z$  axis (at  $10^\circ$ ). The next two bands at  $3058$  and  $3054\text{ cm}^{-1}$  have transition moments polarized at  $30\text{-}40^\circ$  from the  $y$  axis. Calculated bands at  $3040$  and  $3032\text{ cm}^{-1}$  are assigned to the experimental band observed around  $3040\text{ cm}^{-1}$  and are calculated to lie about  $18\text{-}19^\circ$  from the  $z$  axis. The lowest energy aromatic C-H stretching band is calculated to lie at  $3029\text{ cm}^{-1}$  and has an intensity 1-2 orders of magnitude smaller than the other bands in this region. This is assigned to a weak band not observed in our spectra but known in the spectra of some 1-alkylnaphthalenes near  $3010\text{ cm}^{-1}$ .<sup>15</sup>

There are no bands between the C=O stretching frequencies calculated at  $1812\text{-}1781\text{ cm}^{-1}$  (observed between  $1738\text{-}1698\text{ cm}^{-1}$ ) and the next group of four well-separated aromatic ring bands from  $1620$  to  $1505\text{ cm}^{-1}$ , which are all known in the spectra of both naphthalene and 1-substituted naphthalenes.<sup>14</sup> This simplifies and nicely secures the ring band assignments in this region despite the large discrepancy between the calculated and experimental C=O stretching frequencies as seen in Figure 4B in the main text. In Figure 4D, a weak band calculated at  $1619$

$\text{cm}^{-1}$ , with a transition moment  $19^\circ$  from the  $y$  axis, is assigned to the band at  $1620\text{ cm}^{-1}$  in the spectrum of **1** in KBr. This band is not observed above the noise in the monolayer spectra. The next band at  $1592\text{ cm}^{-1}$  with a transition moment polarized  $22^\circ$  from the  $z$  axis is observed in all of the spectra around  $1590\text{ cm}^{-1}$ . A third band at  $1565\text{ cm}^{-1}$  is calculated to lie  $12^\circ$  from the  $z$  axis and is assigned to the band observed near  $1570\text{ cm}^{-1}$ . The most intense ring band in this region is calculated at  $1505\text{ cm}^{-1}$  with a calculated polarization  $30^\circ$  from the  $y$  axis.

Some of the most intense calculated ring vibrations fall between  $1500$  and  $900\text{ cm}^{-1}$  (Figure 3 and Table 2 in the main text), a region which is crowded with alkyl C-H deformation bands and  $\text{SiO}_2$  bands (in the monolayer spectra). Intense bands calculated at  $1146$ ,  $1035$ , and  $981\text{ cm}^{-1}$  match well with experimental bands observed in the monolayer spectra at  $1152$ - $1146$ ,  $1025$ , and  $990\text{ cm}^{-1}$ , respectively, but these bands are not conducive to deconvolution for reasons discussed in the previous section. All of the calculated bands in this region agree well with the literature on naphthalene and 1-substituted naphthalenes,<sup>8b,13,14</sup> supporting our choice of scaling factors for this complex region of the spectrum.

Most of the bands between  $900$  and  $750\text{ cm}^{-1}$  are associated with the naphthalene ring, which simplifies correlation of the calculated and experimental spectra shown in Figure 4D. Three bands due to the COOH and  $\text{CH}_2$  groups between  $854$ - $846\text{ cm}^{-1}$  are probably not scaled correctly as there is no band structure in this region in the experimental spectra of **2** (not shown) or **2a** (Figure 3 in the main text) nor any known COOH bands in this region. It is likely that these bands belong between  $950$  and  $900\text{ cm}^{-1}$ , where acid O-H deformation bands have been reported,<sup>8c</sup> and these are the only calculated bands not listed in the order of decreasing energy in Table 2 in the main text.

The first calculated ring band below  $900\text{ cm}^{-1}$  is a very weak oop polarized band at  $860\text{ cm}^{-1}$ . We did not observe this in any of our experimental spectra, but a weak oop band between  $865\text{--}851\text{ cm}^{-1}$  has been identified in several 1-alkylnaphthalenes.<sup>14,15</sup> A relatively strong band calculated at  $829\text{ cm}^{-1}$  with a transition moment  $19^\circ$  from the  $z$  axis is assigned to the intense band around  $833\text{ cm}^{-1}$  in the experimental spectra. It appears that a second band of different polarization may be present on the high energy side of this band, around  $840\text{ cm}^{-1}$ , given the similar structure in the monolayer spectra and the difference in bandwidth between the monolayer and KBr spectra. A medium intensity band has been observed<sup>17</sup> in this region in the spectra of several *n*-alkanes longer than heptane and assigned to methylene twisting and rocking. Given the incomplete treatment of the chain in our calculations, it is plausible that we missed a relatively intense band here.

Two intense bands calculated to be of mixed origin but primarily due to Si-O-C stretching fall at  $815$  and  $786\text{ cm}^{-1}$  (Figure 4D), coincident with bands in the spectrum of **5** (although the calculated intensities show the opposite relative values from those observed). While we could not find a definitive assignment for these bands in the literature, similar bands have been observed in IR spectra of related trialkoxysilanes and decrease in intensity with polymerization and concomitant loss of the alkoxy groups.<sup>18</sup> We have attempted to subtract out the contribution from these bands as described above. At  $799$  and  $789\text{ cm}^{-1}$ , a relatively intense oop band and a band polarized  $4^\circ$  from the  $y$  axis, respectively, are assigned to the experimental band around  $798\text{ cm}^{-1}$ . The structure in this band and different bandwidths observed in the KBr and mixed monolayer spectrum support this band being of mixed polarization. The calculated band at  $776\text{ cm}^{-1}$  with an oop polarized transition moment is assigned to the band observed at the same

frequency in all of the experimental spectra. Three strong bands have been identified<sup>15</sup> in the spectra of several 1-alkylnaphthalenes at 800, 795-790, and 776-770  $\text{cm}^{-1}$ , and typically appear as a doublet at 800 and 780  $\text{cm}^{-1}$ . While the assignments of the first two intense experimental bands in this region remain somewhat ambiguous due to mixing and decidedly different bandwidths in the KBr and monolayer spectra, the oop assignment of the band at 776  $\text{cm}^{-1}$  seems to be secure.

The DFT/B3LYP/6-31G(d,p) calculated spectrum of propene was found to be in excellent agreement with prior MP2/CCSD/6-311G(d,p) calculations.<sup>4</sup> Directions of the calculated in-plane transition moments in the molecular framework agreed in 12 out of 14 cases and the absolute values of the angles were quite close in all cases. While there were some discrepancies between our calculations and the experimental LD spectrum of propene, the agreement is comparable to that obtained previously,<sup>4</sup> where for intense transitions an uncertainty of  $\pm(5-10)^\circ$  in the calculated transition moment directions was estimated.

### **Fitted Spectra**

The spectrum of **2a** and also that of a polycrystalline isotropic sample of  $\text{C}_{20}\text{H}_{42}$  in pressed KBr<sup>19</sup> were fitted with eight Lorentzians as shown in Figure 1S.

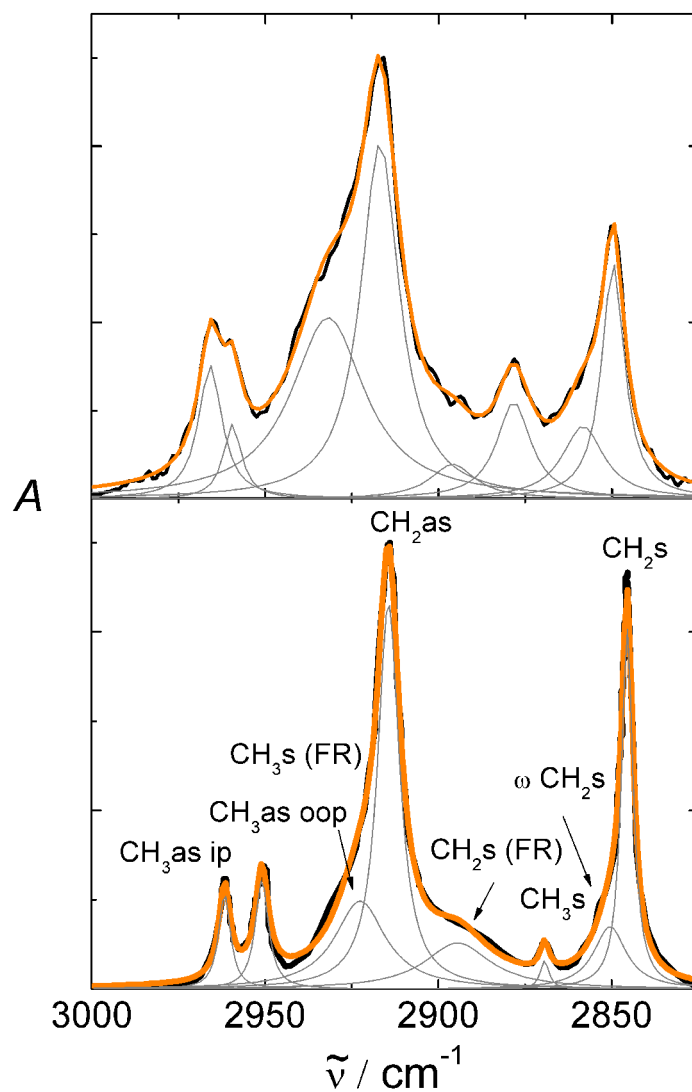


**Figure 1S.** FT-IR spectrum (black line), fitted curves (gray line), and sum of the fitted curves (orange line), for (top) RT **1a** on SiO<sub>2</sub> at RT and (bottom) C<sub>20</sub>H<sub>42</sub> at 9 K, digitally reproduced from Ref. 19. The label FR designates a Fermi resonance band.

## References

1. *AutoEl-II Automatic Ellipsometer Instruction Manual*, 1982. See also: Tomkins, H. G.; McGahan, W. A. *Spectroscopic Ellipsometry and Reflectometry: A User's Guide*; John Wiley & Sons: Canada, 1999, p. 66.
2. Lakowicz, J. R. *Principles of Fluorescence Spectroscopy*, 2<sup>nd</sup> Edition; Kluwer Academic/Plenum Publishers: New York, NY, 1999, p. 52.
3. Gallivan, J. B.; Brinen, J. S.; Koren, J. G. *J. Mol. Spectrosc.* **1968**, 26, 24.
4. Radziszewski, J. G.; Downing, J. W.; Gudipati, M. S.; Balaji, V.; Thulstrup, E. W.; Michl, J. *J. Am. Chem. Soc.* **1996**, 118, 10275.
5. Snyder, R. G.; Strauss, H. L.; Elliger, C. A. *J. Phys. Chem.* **1982**, 86, 5145.
6. Gericke, A.; Huhnerfuss, H. *J. Phys. Chem.* **1993**, 97, 12899.
7. Gericke, A.; Huhnerfuss, H. *Thin Solid Films* **1994**, 245, 74.
8. Socrates, G. *Infrared Characteristic Group Frequencies*, 2<sup>nd</sup> Edition; Wiley: New York, NY, 1994, a) p. 34. b) p. 128. c) Ch. 11. d) p. 192. e) p. 92.
9. Peng, J.B.; Barnes, G.T.; Gentle, I.R. *Adv. Coll. Interface Sci.* **2001**, 91, 163.
10. Ahn, D. J.; Franes, E. I. *J. Phys. Chem.* **1992**, 96, 9952.
11. Tao, Y-T.; Lee, M-T.; Chang, S-C. *J. Am. Chem. Soc.* **1993**, 115, 9547.
12. Song, Y. P.; Petty, M. C.; Yarwood, J. *Langmuir* **1993**, 9, 543.
13. Friedman, H. M. *Appl. Spectrosc.* **1970**, 24, 44.
14. Michaelian, K. H.; Ziegler, S. M. *Appl. Spectrosc.* **1973**, 27, 13.
15. Wilberly, S. E.; Gonzalez, R. D. *Appl. Spect.* **1961**, 15, 174.
16. Olsen, J. E.; Shimura, F. *J. Appl. Phys.* **1989**, 66, 1353.
17. Snyder, R. G.; Schachtschneider, J. H. *Spectrochim. Acta.* **1963**, 19, 85.



18. Hoffman, F.; Güngerich, M.; Klar, P. J.; Fröba, M. *J. Phys. Chem. C* **2007**, *111*, 5648.
19. MacPhail, R. A.; Strauss, H. L.; Snyder, R. G.; Elliger, C. A. *J. Phys. Chem.* **1984**, *88*, 334.